Supplementary Material and Methods

REAGENTS or RESOURCES	SOURCE	IDENTIFIER
Antibodies		
Mouse monoclonal anti-E-cadherin	BD Bioscience	Cat# 610181; RRID: AB_397580
Rabbit monoclonal anit-YAP	Cell Signaling Technology	Cat# 14074; RRID: AB_2650491
Rabbit polyclonal anti-Cleaved Caspase3	Cell Signaling Technology	Cat# 9661; RRID: AB_2341188
Rabbit monoclonal anti-Ki67	Thermo Fisher Scientific	Cat# 9106; RRID: AB_331768
rabbit polyclonal anti-H3K4me1	Millipore	Cat# 07-436; RRID: AB_10068114
rabbit polyclonal anti-H3K4me2	Millipore	Cat# 07-030; RRID: AB_310342
rabbit polyclonal anti-H3K4me3	Cell Signaling Technology	Cat# 9727; RRID: AB_561095
Rabbit monoclonal non-phosphorylated-YAP	Abcam	Cat# 205270; RRID: N/A
Rabbit monoclonal anti-NICD	Cell Signaling Technology	Cat# 4147; RRID: AB_2153348
Mouse monoclonal anti-tubulin	Sigma Aldrich	Cat# T9026; RRID: AB_477593
Mouse monoclonal anti-p53	Millipore	Cat# OP43-20UG; RRID: AB_564968
Rabbit monoclonal anti-Mll1	Cell Signaling Technology	Cat# 14197; RRID: AB_2688010

Rabbit monoclonal anti-hMll2	Cell Signaling Technology	Cat# 63735; RRID: AB_2737357
Rabbit monoclonal anti-Wdr5	Cell Signaling Technology	Cat# 13105; RRID: AB_2620133
Rabbit monoclonal anti-Ash2l	Cell Signaling Technology	Cat# 5019; RRID: AB_1950350
Rabbit polyclonal anti-Erk1/2	Cell Signaling Technology	Cat# 9102; RRID: AB_330744
Mouse monoclonal anti-pErk1/2	Sigma Aldrich	Cat# M9692; RRID: AB_260729
Mouse monoclonal anti-Mek1	Cell Signaling Technology	Cat# 4694; RRID: AB_10695868
Rabbit monoclonal anti-pMek1	Cell Signaling Technology	Cat# 9154; RRID: AB_2138017
isotype IgG control	Cell Signaling Technology	Cat# 3900 ; RRID: AB_1550038
Rabbit polyclonal anti-Mll2	[1]	N.A.
Donkey anti-rabbit-Cy3	Dianova	Cat# 111-165-144; RRID: AB_2338006
Donkey anti- rabbit -Cy3	Dianova	Cat# 711-546-152; RRID: AB_2340619
Donkey anti-mouse-AlexaFluor 488	Dianova	Cat# 715-545-151; RRID: AB_2341099
Anti-rabbit-HRP-conjugated	Agilent	Cat# K4003; RRID: AB_2630375
goat-anti-rabbit-HRP-conjugated	Dianova	Cat# 111-035-144; RRID: AB_2307391
goat-anti-mouse-HRP-conjugated	Dianova	Cat# 115-035-062; RRID: AB_2338504

Chemicals, Peptides, and Recombinant Proteins		
Matrigel	Corning	Cat# 356231
Wnt3a	R&D	Cat# 1324-WN
Y-27632	Sigma Aldrich	Cat# A9165
Tryplex	GIBCO	Cat# 12563
MI-2	Selleckchem	Cat# S7618
Verteporfin	Sigma Aldrich	Cat# SML0534
SCH772984	Selleckchem	Cat# S7101
DAPT	Sigma Aldrich	Cat# D5942
U0126	Calbiochem	Cat# 662005
PP2	Sigma	Cat# P0042
XMU-MP-1	TargetMol	Cat# T4212
mEGF	Gibco	Cat# PMG8043
mNoggin	Peprotech	Cat# 250-38
hR-Spondin1	Peprotech	Cat# 120-38
hEGF	Invitrogen	Cat# PHG0311

hNoggin	Peprotech	Cat# 120-10
sWnt	U-Protein Express	Cat# N001
SB202190	Sigma Aldrich	Cat# S7067
A83-01	Merck	Cat# 616454
CHIR-99021	Selleckchem	Cat# S1263
Primocin	Invivogen	Cat# ant-pm
4-hydroxy-tamoxifen	Sigma Aldrich	Cat# 94873
AdvancedDMEM/F12	Gibco	Cat# 12634-010
AdvancedDMEM	Gibco	Cat# 12491-015
F12 medium	Gibco	Cat# 31765-027
N-Acetylcysteine	Gibco	Cat# A9165
GlutaMax	Gibco	Cat# 35050-038
Nicotinamide	Sigma	Cat# N0636
HEPES	Gibco	Cat# 15630-056
N2	Gibco	Cat# 17502048
B27	Gibco	Cat# 17504
cOmplete (protease inhibitor)	Sigma Aldrich	Cat# 11836170001
Phosphatase inhibitor 2	Sigma Aldrich	Cat# P0044
Phosphatase inhibitor 3	Sigma Aldrich	Cat# P5726

Transdux	SBI-System Bioscience	Cat# LV850 A-1
doxycycline	LKT Laboratories,	Cat# D5897
immo-mount	Thermofisher	Cat# 9990402
Lenti-X Concentrator	Takara	Cat# 631231
PEI	Polyscience Europe	Cat# 24765-2
Dynabeads	Sigma Aldrich	Cat# 10003D
Experimental Models: Organisms/Strains		
Mouse B6: *VillinCre^{ERT2}; NICD$^{flox/flox}$; p53$^{flox/flox}$*	[2]	N/A
Human cancer organoids	[3, 4]	N/A
Human naïve wt organoids	[5]	N/A
Oligonucleotides		
shRNA for knockdown, suppl. table 1	[6]	N/A
Primers for RT-qPCR, suppl. table 2	This study and [7, 8]	N/A
Vector/Plasmids		
pInducer11	[9]	Addgene: 44363
pInducer20	[9]	Addgene: 44012
pInducer11-shMll1	This study	N/A
pInducer11-shYap (1)	This study	N/A

pInducer11-shYap (2)	This study	N/A
Deposited Data		
RNA-seq data	This paper	E-MTAB-6588
YAP targets	[10]	
intestinal stem cell signature	[11]	
Cell type specific signature (goblet, Paneth and enterocytes)	*12*	
Enteroendocrine gene set	GO:0035883	
Fetal/regenerative signature	[13, 14]	
Critical Commercial Assays		
TruSeq stranded mRNA library preparation k	Illumina	20020594
pENTR/D-TOPO Cloning	Invitrogen	Cat# K240020
Software and Algorithms		
R		R v3.4
consensusPathDB webtool		http://cpdb.molgen.mpg.de/MCPDB
FASTQC		Andrews S. (2010). FastQC: a quality control tool for high throughput sequence data. Available online at: http://www.bioinformatics.babraham.ac.uk/projects/fastqc
STAR aligner		https://www.ncbi.nlm.nih.gov/pubmed/23104886
DESeq2		RRID:SCR_015687; https://genomebiology.

		biomedcentral.com/articles/10.1186/s13059-014-0550-8
featureCounts software		Liao Y, Smyth GK and Shi W. featureCounts: an efficient general-purpose program for assigning sequence reads to genomic features. *Bioinformatics*, 30(7):923-30, 2014
Fiji imageJ	https://fiji.sc/	N/A
Imaris 8	Bitplane	N/A
GraphPadprims	GraphPad	N/A

Organoid culture

All mice were bred in pathogen-free conditions, and care and use of animals were performed according to the European and National regulations, published in the Official Journal of the European Union L 276/33, September 22, 2010.

The mice have been previously described in [2]. Dissected small intestines of *VillinCre^{ERT2}; NICD$^{flox/flox}$; p53$^{flox/flox}$* mice were washed with cold PBS and opened longitudinally. Villi were reduced by scraping the intestinal inside with a glass coverslip. The small intestines were cut into 5mm pieces and washed with cold PBS until the supernatant was clear. Pieces were transferred to 8mM EDTA/PBS for 5 min at RT prior to 20 min incubation in 2mM EDTA/PBS on a wheel at 4°C. By careful pipetting and shaking, the epithelia were dissociated from the intestinal pieces, and crypt-enriched fractions were collected. Selected fractions were washed once with 0.1% BSA/PBS and applied onto a 70 µm filter. 200 crypts were seeded in 25 µl of growth factor-reduced Matrigel (BD Matrigel #356231) in a 48-well plate. The basic crypt medium consisted of 60/40 AdvancedDMEM/F12 medium supplemented with N2 and B27, HEPES, GlutaMax, N-Acetylcysteine and Penicillin/Streptomycin (Gibco). The medium to culture control organoids was further supplemented with final concentrations of 50ng/ml mEGF (Gibco, PMG8043), 100 ng/ml mNoggin (Peprotech, 250-38) and 200ng/ml hR-Spondin1 (Peprotech, 120-38). Organoids were split every 6 days by mechanical dissociation with a BSA-coated fire-polished Pasteur pipette. Cre-mediated recombination was induced by 400nM 4-hydroxy-

tamoxifen (Sigma, 94873) for 1 day. *NICD/p53*$^{-/-}$ organoids were further cultured with basic crypt medium (see above) and split every 3-4 days by single-cell suspension with 3 min incubation in TripLE (Invitrogen) at 37°C, followed by washing with 0.1% BSA/PBS. Organoids were treated with 0.5-2.5 µM of Verteporfin, VP (SML0534, Sigma), 0.05-1.5 µM Menin inhibitor, MI-2 (S7618, Selleckchem), 100-500 nM SCH772984 (S7101, Selleckchem), 10µM U0126 (Calbiochem), 15µM DAPT (D5942, Sigma) for the indicated times.

The human wt organoid culture has been previously described [5]. In brief, human colon organoid lines were cultured in Advanced Dulbecco's Modified Eagle's Medium/F12 (#12634,Gibco) containing 10 mM HEPES, 2 mM GlutaMAX, 1.25 mM N-acetylcysteine and 25% R-spondin1 conditioned medium, 1x B-27, 1x N2, 500 nM A83-01, 1 mM nicotinamide and 100 µg/ml primocin (#ant-pm, Invivogen) was supplemented with (N0636, Sigma), 10 µM SB202190 (#S7067, Sigma), 3 µM CHIR-99021 (#S1263, Selleckchem), 0.328 nM sWnt (#N001, U-Protein Express), 50 ng/ml hEGF (#PHG0311, Invitrogen) and 100 ng/ml hNoggin (#120-10C, Peprotech).

Generation of lentiviral particles

For doxycycline-inducible expression shRNA, in combination with a fluorescent reporter, vectors of the pInducer tool kit were used [9]. shRNAs targeting Yap and Mll1, designed to contain the optimized mir30 backbone (Suppl. table 1, [6]) were subsequently cloned into pInducer10 and pInducer11. For production of lentiviral particles, 293TN cells were co-transfected with 10 µg psPAX2, 2.5 µg pMD2.G and 10 µg lentiviral vector on a 10 cm dish by lipofectation using PEI (Sigma). Supernatants were harvested after 24 and 48 h of transfection and passed through a 0.45 mm diameter pore filter. Viral particles were concentrated with Lenti-X Concentrator (Takara) and re-suspended in basic crypt medium.

Infection of organoids with lentiviral particles

Organoids were isolated from Matrigel, washed, dissociated with TripLE, and washed again with 0.1% BSA/PBS. Supernatant was removed and cells were re-suspended and mixed with viral particles in basic crypt medium supplemented with 200 ng/ml hRspo1 (Peprotech), 400 µM hWnt3a, 10 mM nicotinamide, 10 µM Y27632 and transdux (System Bioscience), and transferred to a polyhema-coated 48-well dish and spin-occulated for 45 min at 1000 rpm before incubation for 5 h in the cell culture

incubator. Infectious cell solutions were washed with 1 ml of 0.1% BSA/PBS, seeded in Matrigel and cultured in basic crypt medium for 1 day before selection with 1µg/ml puromycin or 200 µg/ml G418. Stable organoids were induced by 600 ng/ml doxycycline (LKT Laboratories, D5897).

Histology and immunohistochemistry staining and analysis

Organoids were fixed with ice-cold 4 % formalin-PBS solution for 1 h, either in Matrigel for whole-mount staining or processed for paraffin-embedding in 1.5 % agarose. The pieces of agarose were dehydrated in ethanol and toluol before transfer into paraffin. Formalin fixed and paraffin-embedded tumor samples were kindly provided by Robine and Louvard [2]. 5 µm sections of paraffin-embedded samples were de-paraffinized and rehydrated before being subjected to antigen retrieval with 20 mM Tris pH 8.5 and 1 mM EDTA by boiling for 18 min. For immunohistochemistry, sections were incubated for 5min in 4% H2O2/PBS before 1h incubation with blocking solution (0.1% Tween, 10% horse serum in PBS) and for immunofluorescence staining, slides were incubated for 1 h with a blocking solution (0.1% TritonX, 10% horse serum in PBS) followed by overnight incubation of the primary antibody at 4 °C. After washing with 0.1 % Tween/PBS, slides for immunofluorescence were incubated with fluorochrome-conjugated secondary antibodies and 4′,6-diamidino-2-phenylindole for 1 h and mounted in immo-mount (Thermofisher). For immunohistochemistry slides were incubated with HRP-conjugated antibody and developed with a chromogenic substrate (DAB) according to the manufacturer□s protocol (DAKO), and counterstained with hematoxylin staining.

Light microscopy and data analysis

Growth of individual organoids was tracked with a Leica DIM6000 microscope equipped with an NPlan 10x NA 0.25 or NCX FLPlan 5x NA 0.12 objective and a motorized LMT200 V3 High precision Scanning Stage to relocate previously stored positions.

Representative z-stacks from immunofluorescence procedures were acquired with either an inverted laser scanning microscope LSM710 using an 405 nm, 488 nm and 561 nm laser and an PlanApochromat 20x NA 0.8 objective (Zeiss Jena, Germany) and voxel size of 0.19µm x 0.19µm x 0.73µm or a spinning disc confocal microscope CSU-W1 (Nikon/Andor) equipped with an iXON888 camera, using PlanApo 20x NA

0.75 and Apo LWD 40x NA 1.15 objectives. For quantifications, complete z-stacks of the organoids without intensity saturations were acquired under identical conditions.

Images were analyzed with Fiji and Imaris 8 (Bitplane/Andor) software. The Fiji ROI manager plugin was used to quantify the growth of the organoids over time. To quantify the mean fluorescence intensity of the specified signals in the 3D reconstructed organoids, segmentation in the Surface module of Imaris was used by selection of nuclear fluorescence in a mask created with the DAPI channel.

Graphs and statistics were generated with GraphPad Prism. Tests for normal distribution were performed with D'Agostino-Pearson and Shapiro-Wilk tests: data were shown in a boxplot, and significance (p value) was determined with Mann-Whitney test (two-tailed) or students T-test.

Electron Microscopy

Organoids were fixed in 2 % (w/v) formaldehyde and 2.5 % (v/v) glutaraldehyde in 0.1 M phosphate buffer for 2 h at room temperature. After embedding in 10 % gelatin, samples were post-fixed with 1 % (v/v) osmium tetroxide, dehydrated in a graded series of ethanol, and embedded in PolyBed® 812 resin (Polysciences, Germany). Ultrathin sections (60-80 nm) were stained with uranyl acetate and lead citrate, and examined at 80 kV with a Morgagni electron microscope (FEI, Holland). Acquisition of pictures was done with a Morada CCD camera and the iTEM software (Emsis GmbH, Germany).

Western blots

Organoids were harvested and washed once in ice-cold 0.1% BSA/PBS followed by two washings in ice-cold PBS. Cells were lysed in RIPA buffer (50mM Tris, pH8, 150mM NaCl, 0.1 % SDS, 1 % NP40, 0.5 % Deoxycholate), extracts were separated on 10 % polyacrylamide gels and transferred to a nitrocellulose membrane via semidry transfer (25 mM Tris, 192mM glycine, 20% methanol, pH 8,3). For detection of large proteins, such as Mll1 and mMll2, proteins were transferred to a nitrocellulose membrane via wet transfer (25 mM Tris, 192mM glycine, 0.35mM SDS, 20% methanol).

Co-immunopreciptiation

Organoids were harvested and 5x washed in ice cold PBS before lysis in IP-buffer (139 mM KCl, 12 mM NaCl, 0.8 mM MgCl2, 20 mM Tris- HCl [pH7.5], 0.5% IGEPAL

CA-630, 0.2 mM EDTA, 20% [v/v] glycerol, 1 mM DTT, protease and phosphatase inhibitors. After brief sonication, benzonase (25U/ml) was added and incubated for 10min on ice, followed by 10min centrifugation (14000rpm, at 5°C). 400µg of organoid protein lysate in total volume of 300µl was incubated with 0.5µg Mll1 or Yap antibody (NEB: 14197S (Clone D6G8N), NEB:14074S (Clone D8H1X)) and isotype IgG control (NEB: 3900 (DA1E)) over night. 20µl Dynabeads (Thermofisher) was washed three times, and after 1h blocking in 0.1% BSA/PBS lysates were added and incubated at 4°C rotating for 4h. Dynabeads were washed 5 times with lyses buffer and finally cooked for 5min at 96°C with SDS-Page loading buffer.

qRT-PCR and RNA-sequencing

Organoids were harvested and washed with 0.1 % BSA/PBS, and total RNA was isolated using Trizol extraction (Invitrogen). DNA contaminations were removed by DNase1 digestion (Invitrogen) in the presence of Rnase Inhibitor (RNase Out, Invitrogen), followed by RNA purification via phenol/chloroform extraction.

For qRT-PCR, 5 µg of extracted RNA was reverse-transcribed with random hexamer primers (Invitrogen) and MMLV reverse Transcriptase (Promega, 200U/µl), following the manufacturer's instructions. Quantitative reverse transcription PCR was performed in a total volume of 20 µl SybR green reaction mix (Roche, Diagnostics) containing 0.25 µM of each primer (see suppl. table 2) in a CFX96-C1000T thermal cycler (BioRad). The PCR program included an activation step at 50 °C for 2 min, a denaturation step at 95 °C for 2 min followed by 40 cycles of 95 °C for 15 s, and a combined annealing and elongation step at 60 °C for 1 min. All reactions were performed as quadruplicates. The quantification was performed using the $\Delta\Delta C_t$ method by comparing the expression of the target genes of treated versus control samples, relative to the endogenous reference *GAPDH.* Expression data from MI-2 treatment were relative to the endogenous reference *B2M*. Data are expressed as mean ± SD. Differences between two groups were determined by Student's t-test. $P < 0.05$ was considered significant;*: $p \leq 0.05$, **: $p \leq 0.001$, ***: $p \leq 0.0001$.

To perform mRNA sequencing, RNA was extracted from control and *NICD/p53*$^{-/-}$ organoids, as described above. RNA was collected from two technical replicates of three individual biological replicates. Sequencing libraries were generated using the Illumina TruSeq Stranded mRNA Kit, and samples were processed in two pools with HiSeq 4000 in one run (1 pool - 1 lane). RNA-seq reads were quality-checked by

FASTQC (v0.11.5) software. Sequencing reads were mapped to the mouse whole genome (mm10) using STAR aligner (v. 2.5.3a). Read counts for each gene (gencode vM12) were extracted from the BAM file using featureCounts software (1.5.1). Read counts from different biological groups were subjected to differential expression analysis using the DESeq2 R statistical package. Comparisons between controls and mutants were corrected by individual technical replicates (linear model). In order to avoid background signal/noise, genes with less than 10 reads over all samples were excluded before adjusting the p-value for multiple testing. Genes with adjusted p-value lower than 0.01 and absolute fold-change (log2) higher than 0.4 were considered deferentially expressed. Heatmaps were generated by gplots heatmap.2; before plotting the expression values were log transformed and scaled by z-transformation. Volcano plots were generated with R. Violin plots were generated with ggplot2.violinplot function from ggplot2 R package and tested for the differential expression of cell type specific [29], stem cell [11] and fetal/regenerative gene set [13]. RNA-seq sample files were submitted to ExpressArray (accession number: E-MTAB-6588)

Supplemental tables

Supplemental table 1

shRNA sequences	
targets	*shRNA, 97 oligomer* [6]
hMll1	TGCTGTTGACAGTGAGCGAAAGAAAGATTCTAAAAGTATATAGTGAAGCCACAGATGTATATAC TTTTAGAATCTTTCTTCTGCCTACTGCCTCGGA
mYap	TGCTGTTGACAGTGAGCGCAGGGTTCATAATGAACAACAATAGTGAAGCCACAGATGTATTGT TGTTCATTATGAACCCTTTGCCTACTGCCTCGGA
mYap	TGCTGTTGACAGTGAGCGATAGAACAGAGATGAAATTCTATAGTGAAGCCACAGATGTATAGA ATTTCATCTCTGTTCTACTGCCTACTGCCTCGGA

Suppl. table 1: shRNA sequences: cloned into pInducer10/11

Supplemental table 2

Primers for RT-qPCR			
targets	*Direction*	*Oligo 5□ 3□*	*source*
Gapdh	fwd	AAATGGTGAAGGTCGGTGTGAACG	[7]
Gapdh	rev	TGATGACAAGCTTCCCATTCTCGG	[7]
Beta-microglobulin	fwd	GTTAAGTGGGATCGAGACATGTAAG	This study
Beta-microglobulin	rev	TAGAGCTACCTGTGGAGCAA	This study
Hey1	fwd	TCTTGCAGATGACTGTGGATCACC	This study
Hey1	rev	AGGCATCGAGTCCTTCAATGATGC	This study
Yap	fwd	AAGGCTGGACCCTCGTTTTG	[8]
Yap	rev	TCCGTATTGCCTGCCGAAAT	[8]

Mll1	fwd	GCTCAGATGAAGAAGTCAGAG	(Francis Stewart)
Mll1	rev	GGGAAAACACAGATGGGTCTG	(Francis Stewart)
Mll2	fwd	ATGGTTCCTCAGACCTACTG	(Zhu et al., 2019)
Mll2	rev	TCCACACTGAAGCCATCATC	(Zhu et al., 2019)
Ctgf	fwd	GGGCCTCTTCTGCGATTTC	[8]
Ctgf	rev	ATCCAGGCAAGTGCATTGGTA	[8]
Ankrd1	fwd	GGATGTGCCGAGGTTTCTGAA	[8]
Ankrd1	rev	GTCCGTTTATACTCATCGCAGAC	[8]
Cyr61	fwd	CTGCGCTAAACAACTCAACGA	[8]
Cyr61	rev	GCAGATCCCTTTCAGAGCGG	[8]
Igfbp3	fwd	TCTAAGCGGGAGACAGAATACG	[8]
Igfbp3	rev	CTCTGGGACTCAGCACATTGA	[8]
Lysozyme	fwd	GCAGCCATACAATGTGCAAAGAGG	[7]
Lysozyme	rev	TTTGCCCTGTTTCTGCTGAAGTCC	[7]
ChroA	fwd	AGAAGTGTTTGAGAACCAGAGCCC	[7]
ChroA	rev	TTGGTGATTGGGTATTGGTGGCTG	[7]
Gob5	fwd	TGAAATTGTGCTGCTGACCGATGG	[7]
Gob5	rev	TGCTGCGAAAGCATCAACAAGACC	[7]
Math1	fwd	GTTGCGCTCACTCACAAATAAGGG	[7]
Math1	rev	TGGCAGTTGAGTTTCTTCAAGGCG	[7]
Ascl2	fwd	AAAGCTTGGTCCGGTTCTTCATCC	[7]
Ascl2	rev	GCAGATGCTTAGCTTATTGCGTCC	[7]

Lgr5	fwd	CCTACTCGAAGACTTACCCAGT	[7]
Lgr5	rev	GCATTGGGGTGAATGATAGCA	[7]
Bmi1	fwd	AAAGGTACTTACGATGCCCAGCAG	This study
Bmi1	rev	AAGGTAGTGGGCCATTTCTTCTCC	This study
Tert	fwd	TGAGGTGCAGCGGGATGGGTT	This study
Tert	rev	TCCAGCAGCAAGCCACACCAG	This study
Clu	fwd	AAAGGGGGTGTACTTGAGCAG	This study
Clu	rev	ACCTACTCCCTTGAGTGGACA	This study
Trop2	fwd	GAACGCGTCGCAGAAGGGC	[15]
Trop2	rev	CGGCGGCCCATGAACAGTGA	[15]
Anxa1	fwd	TGATACAGATGCCAGGGCTTT	This study
Anxa1	rev	TCGGCAAAGAAAGCTGGAGT	This study
Spp1	fwd	TCGGAGGAAACCAGCCAAGGACT	[15]
Spp1	rev	AAGCTTCTTCTCCTCTGAGCTGCCA	[15]
Egr1	fwd	ACAACCCTATGAGCACCTGAC	This study
Egr1	rev	GGTCGGAGGATTGGTCATGC	This study
Ly6a	fwd	GCTGATTCTTCTTGTGGCCC	This study
Ly6a	rev	GAGGGCAGATGGGTAAGCAA	This study
hCLU	fwd	TGTTCCACCAACAACCCCTC	This study
hCLU	rev	GGAAGGAACGTCCGAGTCAG	This study
hHEY1	fwd	TGAGAAGCAGGTAATGGAGCAA	This study
hHEY1	rev	CGCTGGGAAGCGTAGTTGTT	This study
hTROP2	fwd	CCAAGTGAGTCACGCTTCCT	This study
hTROP2	rev	CGCTATGCCATCCCTTCCTT	This study

hANXA1	fwd	AGTTCTTTGCAAGAAGGTAGAGA	This study
hANXA1	rev	TGACGCTGTGCATTGTTTCG	This study
hMUC2	fwd	TTTGATGCCAGCATTTGCATCCCG	[7]
hMUC2	rev	TTGGCCGAGTACATGACAAATGTCCC	[7]
hBeta-microglobulin	fwd	GTTAAGTGGGATCGAGACATGTAAG	This study
hBeta-microglobulin	rev	TAGAGCTACCTGTGGAGCAA	This study

Suppl. table 2: primer list; designed and validated primer pairs

References suppl. Information

1. Glaser, S. *et al.* Multiple epigenetic maintenance factors implicated by the loss of Mll2 in mouse development. *Development* **133**, 1423-1432 (2006).
2. Chanrion, M. *et al.* Concomitant Notch activation and p53 deletion trigger epithelial-to-mesenchymal transition and metastasis in mouse gut. *Nat Commun* **5**, 5005 (2014).
3. Boehnke, K. *et al.* Assay Establishment and Validation of a High-Throughput Screening Platform for Three-Dimensional Patient-Derived Colon Cancer Organoid Cultures. *J Biomol Screen* **21**, 931-941 (2016).
4. Schutte, M. *et al.* Molecular dissection of colorectal cancer in pre-clinical models identifies biomarkers predicting sensitivity to EGFR inhibitors. *Nat Commun* **8**, 14262 (2017).
5. Heuberger, J. *et al.* Epithelial response to IFN-gamma promotes SARS-CoV-2 infection. *EMBO Mol Med*, e13191 (2021).
6. Fellmann, C. *et al.* An optimized microRNA backbone for effective single-copy RNAi. *Cell Rep* **5**, 1704-1713 (2013).
7. Heuberger, J. *et al.* Shp2/MAPK signaling controls goblet/paneth cell fate decisions in the intestine. *Proc Natl Acad Sci U S A* **111**, 3472-3477 (2014).
8. von Eyss, B. *et al.* A MYC-Driven Change in Mitochondrial Dynamics Limits YAP/TAZ Function in Mammary Epithelial Cells and Breast Cancer. *Cancer Cell* **28**, 743-757 (2015).
9. Meerbrey, K.L. *et al.* The pINDUCER lentiviral toolkit for inducible RNA interference in vitro and in vivo. *Proc Natl Acad Sci U S A* **108**, 3665-3670 (2011).
10. Gregorieff, A., Liu, Y., Inanlou, M.R., Khomchuk, Y. & Wrana, J.L. Yap-dependent reprogramming of Lgr5(+) stem cells drives intestinal regeneration and cancer. *Nature* **526**, 715-718 (2015).
11. Munoz, J. *et al.* The Lgr5 intestinal stem cell signature: robust expression of proposed quiescent '+4' cell markers. *EMBO J* **31**, 3079-3091 (2012).
12. Haber, A.L. *et al.* A single-cell survey of the small intestinal epithelium. *Nature* **551**, 333-339 (2017).
13. Yui, S. *et al.* YAP/TAZ-Dependent Reprogramming of Colonic Epithelium Links ECM Remodeling to Tissue Regeneration. *Cell Stem Cell* **22**, 35-49 e37 (2018).
14. Wang, P. *et al.* Global analysis of H3K4 methylation defines MLL family member targets and points to a role for MLL1-mediated H3K4 methylation in the regulation of transcriptional initiation by RNA polymerase II. *Mol Cell Biol* **29**, 6074-6085 (2009).
15. Mustata, R.C. *et al.* Identification of Lgr5-independent spheroid-generating progenitors of the mouse fetal intestinal epithelium. *Cell Rep* **5**, 421-432 (2013).

Supplementary figure legends

Suppl. Fig.1: Characterization of NICD/p53$^{-/-}$ mutant organoids

A) Western blot for NICD and p53 from protein lysates of *NICD/p53$^{-/-}$* organoids and controls. B) Brightfield and fluorescence images for NICD-GFP of *NICD/p53$^{-/-}$* organoid 5 days after Cre-mediated recombination. NICD-GFP production in selected *NICD/p53$^{-/-}$* organoid (3D reconstruction, on the right), upper part: Sketch visualizing the generation of *NICD/p53$^{-/-}$* organoid. C) Electron microscopy of NICD/p53-/- organoids shows microvilli at the apical surface on the organoid inside, see also magnification on the right. Inset below and enlargements on the right show cell-cell junctions with interdigitations in the middle, lateral tight-junctions close to the apical side of the organoids and desmosomes (yellow asterisks); scale bar 2µm. D) Confocal immunofluorescence shows strong staining of phalloidin-positive actin at the apical inside of *NICD/p53$^{-/-}$* organoid cells. E) Tracing of control and NICD/p53-/- organoid cultures for 4 days in full medium (ENR) and after growth factor withdrawal (-ENR). F) Organoids of either NICD or p53 mutant organoids in full medium (upper) or after withdrawal of Rspondin (lower). G) Tracing of NICD/p53-/- organoids treated with ICG-001 for three days and assessment of viability by counting growing and normally shaped organoids (on the right). H) Relative expression of secretory cell markers in control and *NICD/p53$^{-/-}$* organoids assessed by qRT-PCR. I) Immunofluorescence staining on sections of formalin-fixed and paraffin-embedded organoids for goblet cells (Intestinal Trefoil Factor, ITF, red arrows), enteroendocrine cells (Chromogranin A, ChroA, green arrow) and Paneth cells (Lysozyme, red arrow); controls in upper panel and *NICD/p53$^{-/-}$* mutants in lower panel; scale bar 50 µm. J) Heat map of stem cell genes differentially regulated in NICD/p53-/- organoids.

Suppl.Fig.2 High nuclear Yap controls growth and viability of NICD/p53$^{-/-}$ tumors and organoids

A) Volcano plot of genes differentially regulated in *NICD/p53$^{-/-}$* organoids with indicated genes downregulated in Yap-expressing organoids. B) Immunohistochemistry for active Yap on paraffin sections of *NICD/p53$^{-/-}$* tumor, scale bar 100µm. C) Brightfield image of 3 day-tracked untreated (upper panel) and 2.5µM Verteporfin (VP) treated *NICD/p53$^{-/-}$* organoids (lower panel), scale bar 250µm. D) Concentration-dependent viability of *NICD/p53$^{-/-}$* organoids treated with VP. E) Yap mRNA expression in shctr and shYap *NICD/p53$^{-/-}$* organoids, assessed by qRT-PCR. F) Left: tracking of individual organoids after doxycycline-induced shRNA knock-down of Yap. After induction, organoids express turboRFP, which shows shRNA production, scale bar 250µm Right: quantification of size increase of individually tracked organoids, normalized to the size of organoids before induction.

Suppl.Fig.3: Stat3 signaling in NICD/p53$^{-/-}$ organoids

A) Volcano plot of genes differentially regulated in *NICD/p53$^{-/-}$* organoids with indicated genes controlled by Stat3. B) Concentration dependent viability of *NICD/p53$^{-/-}$* organoids treated with PP2. C) Western blot of wt small intestinal (upper) and *NICD/p53$^{-/-}$* (lower) organoids upon Src- (PP2, 20µM) or Mst-kinase (XMU-01, 5µM) inhibition. D) Western blot of protein lysates from VP treated *NICD/p53$^{-/-}$* organoids;

Yap inhibition reduced phospho-Erk levels while phosphor-Mek levels remained unchanged. Quantification on the right. E) Relative mRNA expression of Yap target genes, comparing untreated and MAPK inhibitor treated *NICD/p53*$^{-/-}$ organoids.

Suppl.Fig.4: Mll1 in NICD/p53$^{-/-}$ *tumors*

A) Immunofluorescence staining of small intestinal crypt for active Yap, scale bar 30µm. Immunohistochemistry for B) Mll1 and C) H3K4me3 on paraffin sections of *NICD/p53*$^{-/-}$ tumors, scale bar 100µm. D) Western blot of control and *NICD/p53*$^{-/-}$ organoids probed for the histone tri-methyltransferase complex components Mll1, Mll2, Wdr5 and Ash2l. E) Relative mRNA expression of Mll1 and Mll2 in control and *NICD/p53*$^{-/-}$ organoids, assessed by qRT-PCR. F) Scheme of Mll1 and interaction partners in the complex, enzymatic SET H3K4 methyltransferase domain on the right (shown by red arrow below is also the histone tri-methylation), interaction with β-catenin-Tcf4 via CBP in the middle, and Menin-binding domain on the left. Shown is the proteolytically cleaved Mll1, which is disulfide-linked. The Menin inhibitor MI-2 blocks the interaction of Menin with Mll1. G) 3D reconstruction of H3K4me3 (red) and DAPI (blue) in whole-mount immunofluorescence of untreated and MI-2 treated *NICD/p53*$^{-/-}$ organoids; scale bar 20µm, magnifications of insets on the right. Quantification of fluorescence intensities on the far right (n, 500 nuclei of 6 organoids were counted). H,I) Immunofluorescence of; H3K4me1 (red) or H3K4me2 (red) and DAPI (blue), magnification of insets on the right; scale bar 20µm. Quantification of fluorescence intensities at the far right (n, 500 nuclei counted from 6 organoids). J) Immunofluorescence staining on paraffin sections of untreated and MI-2 treated *NICD/p53*$^{-/-}$ organoids for Ki67 and DAPI (red and blue), magnification of insets on the right; scale bar 20µm. Quantification of fluorescence intensities on the far right.

Suppl.Fig.5 High YAP and MLL1 in patient-derived xenografts and organoids

Immunohistochemistry for A) YAP and for B) MLL1 on paraffin sections of patient-derived xenografts (PDX) (n, 8) C) Disease and progression free survival anaylsis (Kaplan-Meier plot) using the Colorectal Adenocarcinoma (TCGA, PanCancer Atlas) and the web-based tool at https://www.cbioportal.org, MLL1 Exp>1.5 or 2, respectively. E) Correlation analysis of TCGA colon cancer expression data for MLL1 and YAP. F) Selection of genes co-expressed with MLL1 in colon cancer, determined by correlation analysis of TCGA colon cancer expression data. G) Brightfield images of human naïve wt (upper) and PDOs (lower) after 4 days treatment with 10µM Nutlin3a (middle) and 10µM Notch inhibitor (DAPT) (right), scale bar 40µm. H) Relative mRNA expression of Notch responsive genes comparing naïve wt and PDOs upon Notch inactivation with DAPT. I) Brightfield images of individual 3 day-tracked untreated (upper panel) and 15 µM DAPT-treated patient-derived organoids (lower panel), scale bar 500µm. J) Western blot from lysates of untreated and DAPT-treated (Notch-inhibited) patient-derived organoids probed for active and total YAP, pErk and Erk. K) Immunofluorescence for MLL1 (green) of patient-derived and wt human organoids, scale bar 50 µm, quantification below (comparison of two individual organoid lines of each condition, and measured a total of 8 organoids).

Suppl. Fig. 6 High YAP and MLL1 in patient-derived organoids

A) Brightfield images of individual 3 day-tracked control (upper) and Verteporfin-treated (lower) patient-derived organoids, scale bar 500µm B) H3K4me3 whole-mount immunofluorescence of untreated and MI-2-treated patient-derived organoids,

quantification of fluorescence intensities on the right (n, >2000 nuclei of organoids were measured). C) Human naïve wt colon organoids untreated (left) and 3 day 1.5μM MI-2 treated (right). D) 24h MI-2 treatment of PDOs reduced Yap target gene expression. E) Non-induced patient-derived organoids (upper two panel) and organoids with doxycycline-induced knock-down of MLL1 (lower two panel) at 1 and 8 days after shMLL1 induction.

A

control
NICD/p53-/-
NICD
p53
Tub.

B

+ 4OHT
single cell dissociation
Organoid
Organoid with spheroid buds
Spheroid
VilCreERT2; P53fl/fl; NICDfl/fl
NICD-EYFP
3D-reconstruction
5 days after Tamoxifen
NICD/p53-/-

D

outside
inside
Phalloidin/ DAPI

C

NICD/p53-/-
inset
Microvilli
Interdigitations
Tight junctions
Desmosome

E

control
NICD/p53-/-
+ ENR
- ENR
day 0
day 4

F

control
NICD
p53-/-
+ENR
+EN

G

day 0
day 1
day 3
ICG-001
+10µM ICG
viable organoids, %
mutant
ICG 10µM
0
24h
48h
72h

H

Lyz
ChgA
Gob5
Math1
relative expression
control
NICD/p53-/-

I

ITF/ChroA/ DAPI
Lys./DAPI
control
NICD/p53-/-

J

stem cell marker expression
Color Key
Value
control
NICD/p53-/-

suppl. Fig. 1, Heuberger et al. 2021

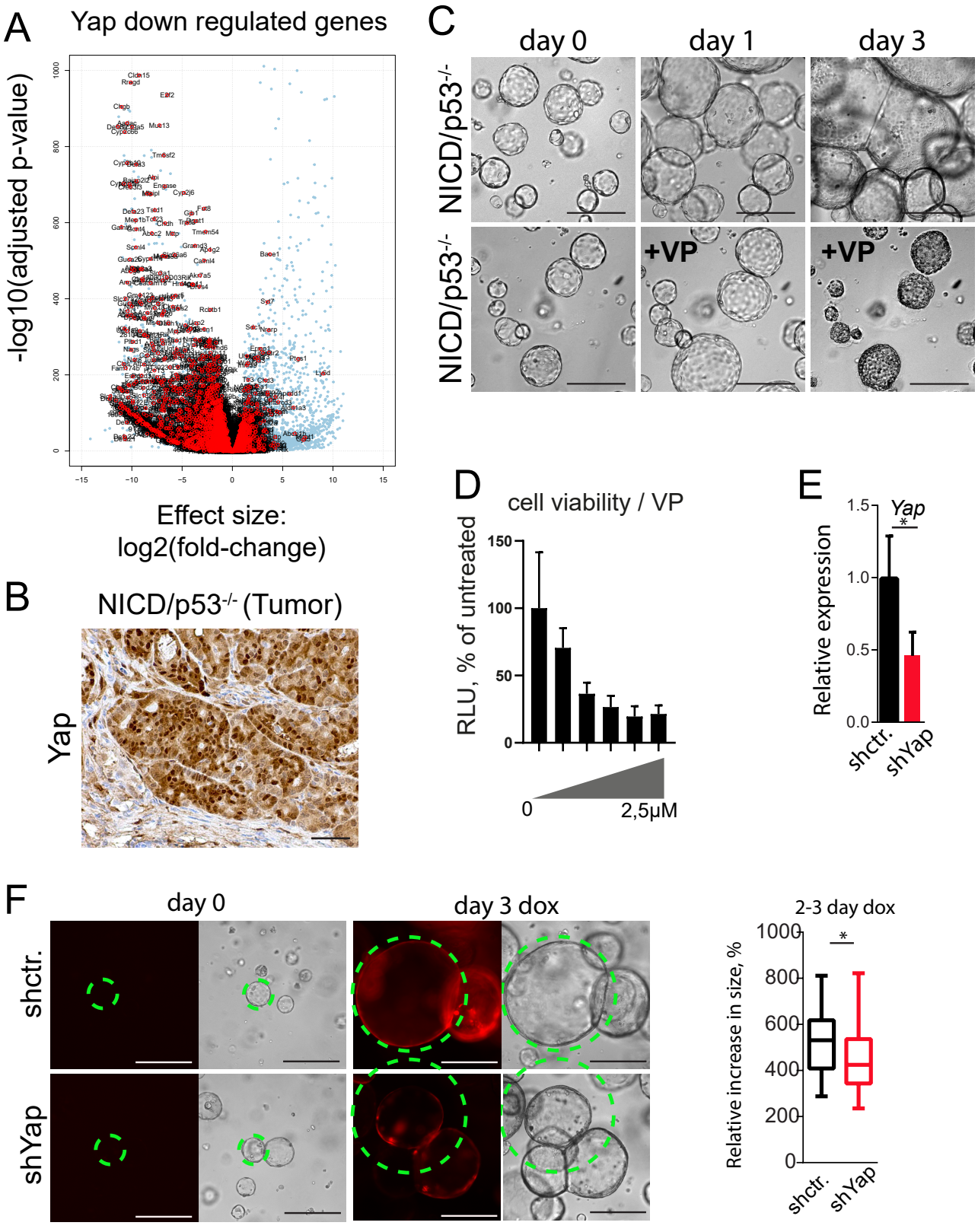

suppl. Fig. 2, Heuberger et al. 2021

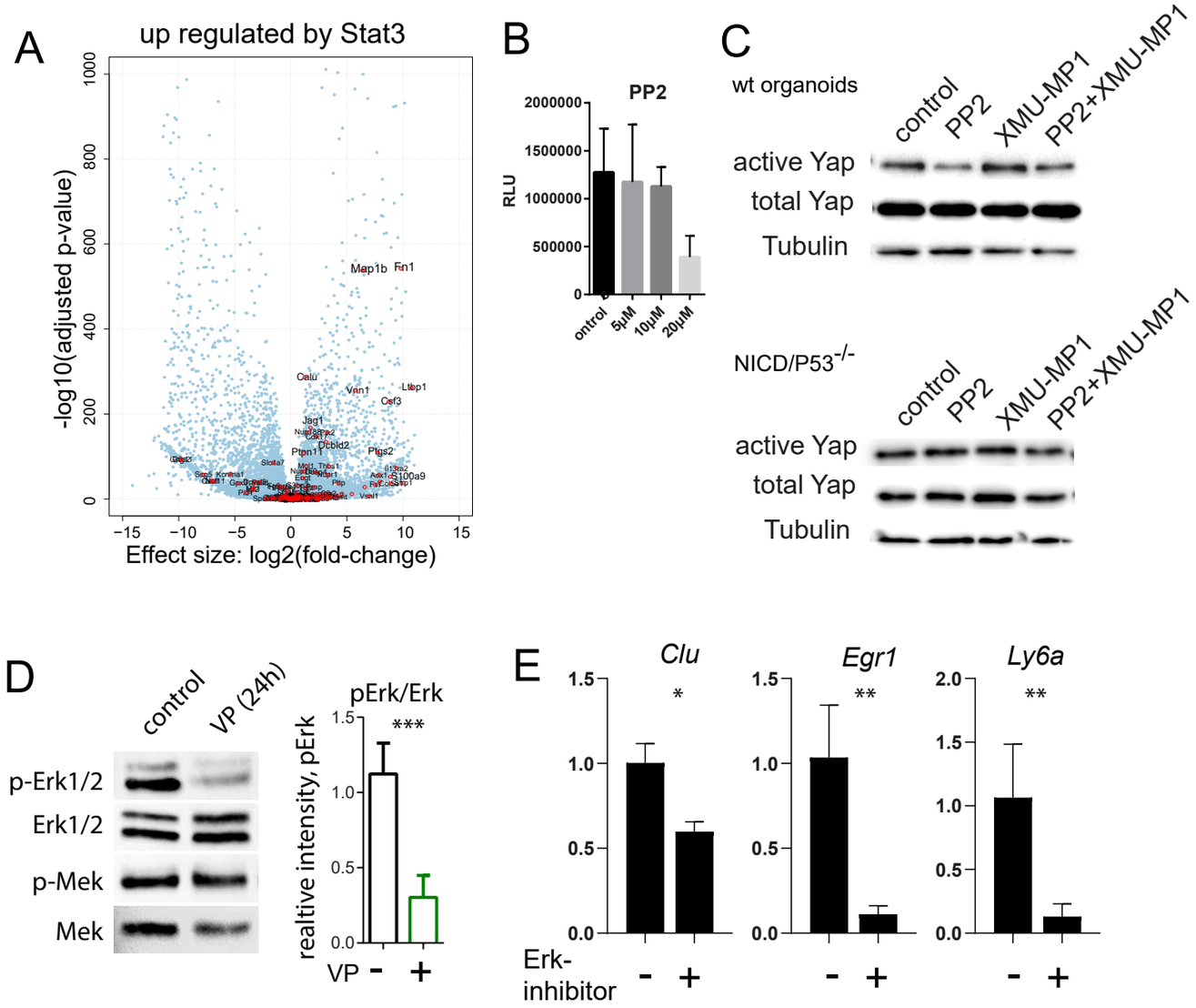

suppl. Fig. 3, Heuberger et al. 2021

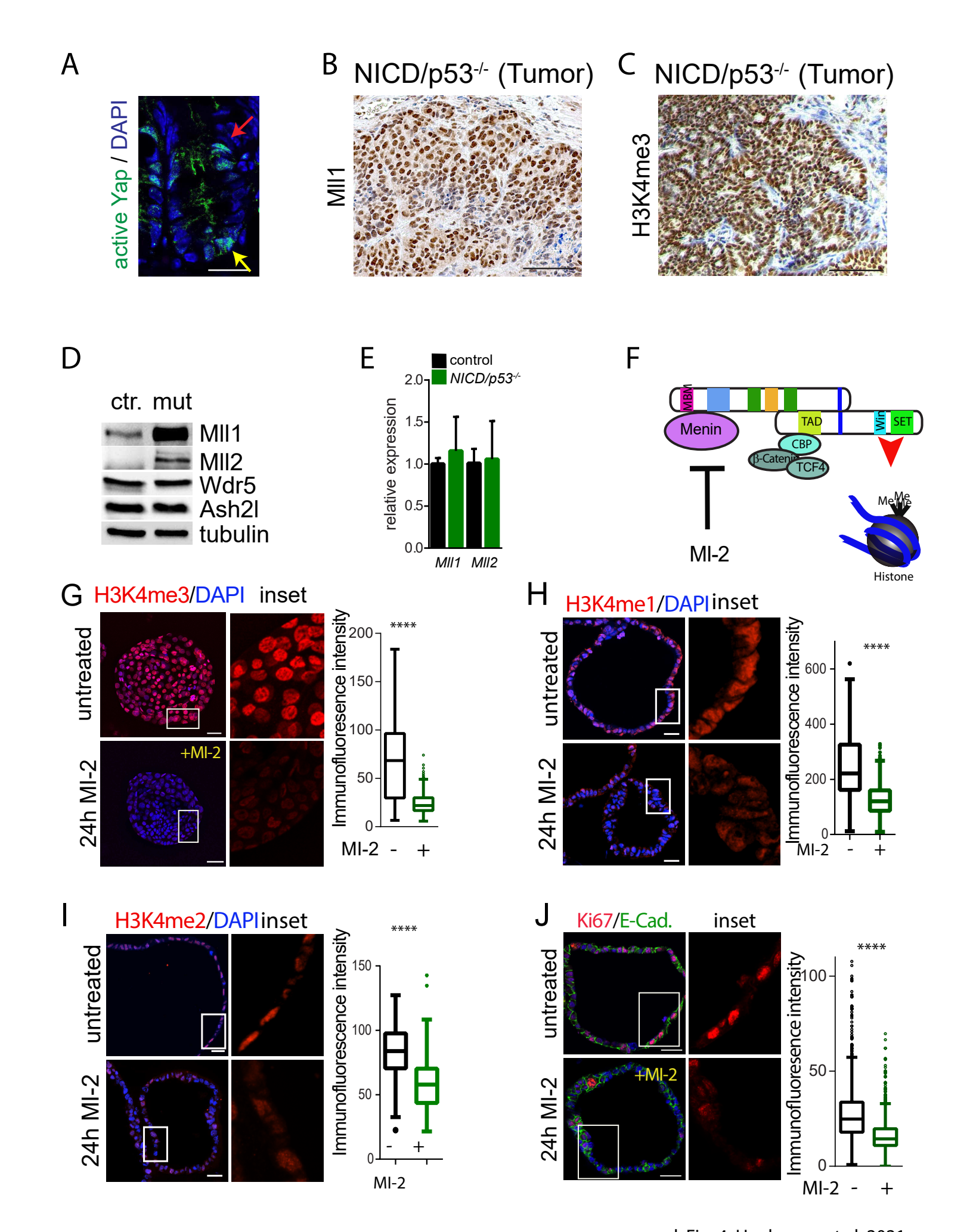

suppl. Fig. 4, Heuberger et al, 2021

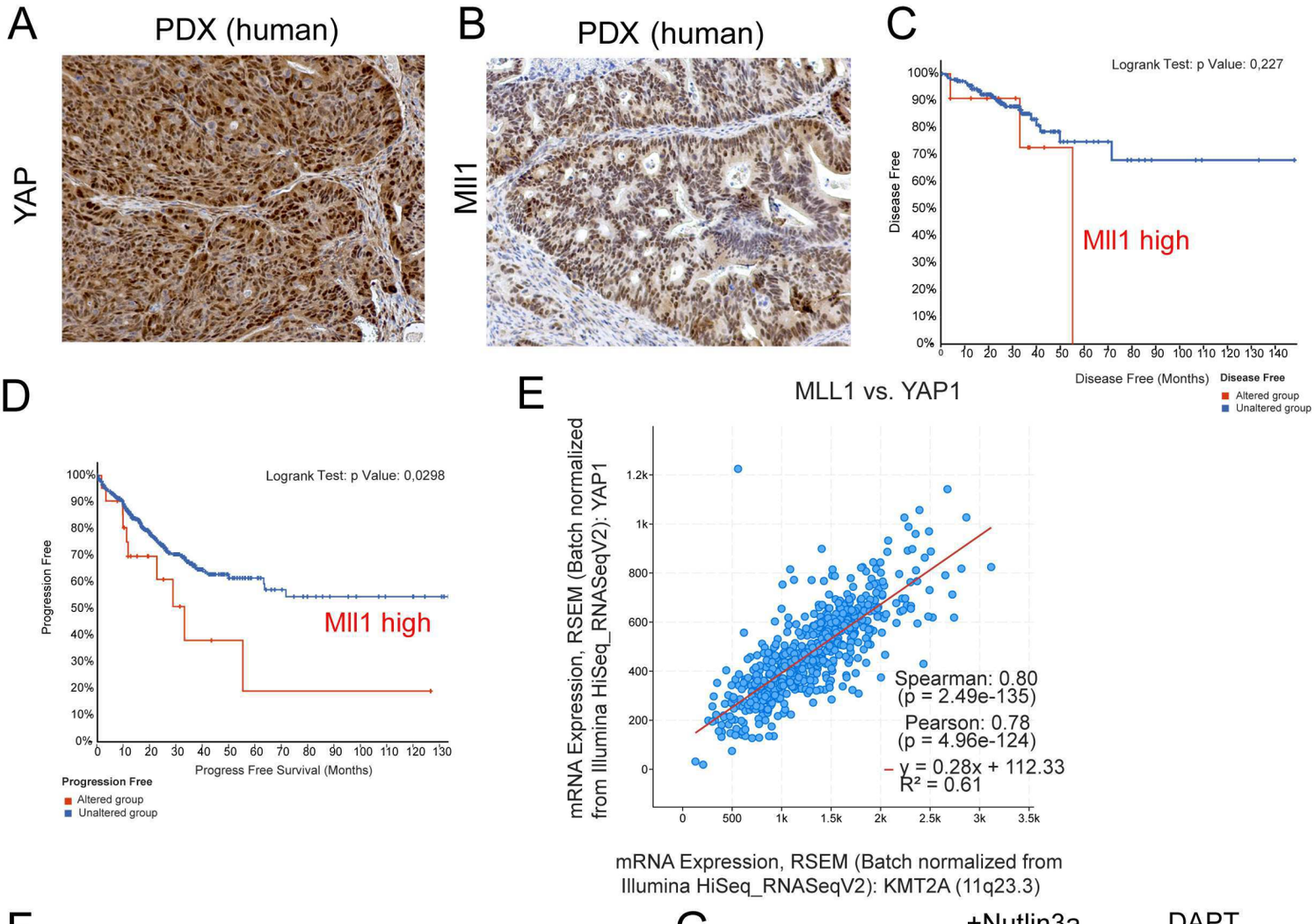

F

Genes co-expressed with MLL1 in CRC

Correlated Gene	Cytoband	Spearman's Correlation	p-Value	q-Value
YAP1	11q22.1	0.360	1.38e-19	1.48e-18
CLU	8p21.1	0.258	1.74e-10	8.01e-10
ANXA1	9q21.13	0.0516	2.10E-01	2.70E-01
TACSTD2	1p32.1	-0.0732	7.53E-02	1.08E-01
SPP1	4q22.1	0.0523	2.04E-01	2.63E-01
HEY1	8q21.13	0.168	4.13E-02	1.00E-01
ANKRD1	10q23.31	0.124	2.52E+00	4.74E+00

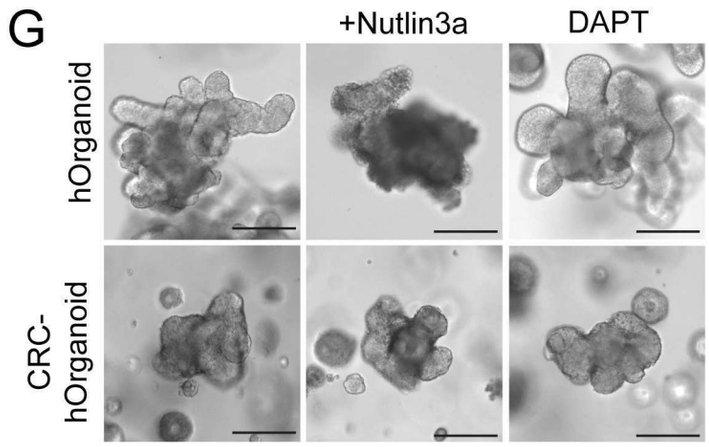

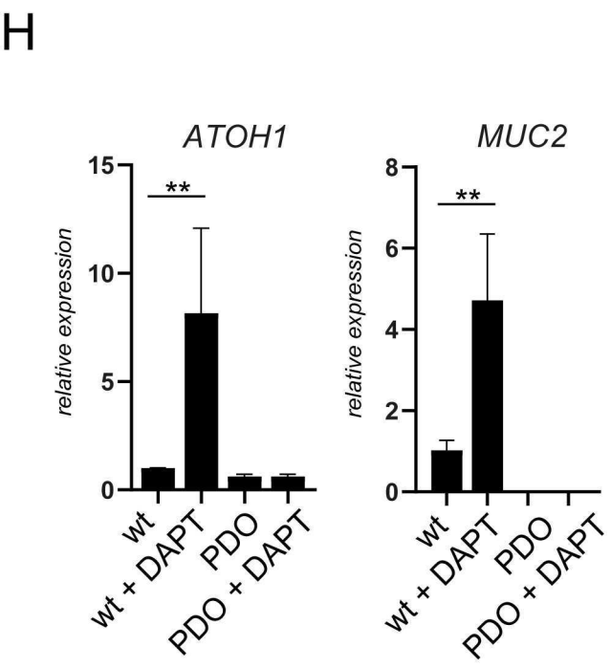

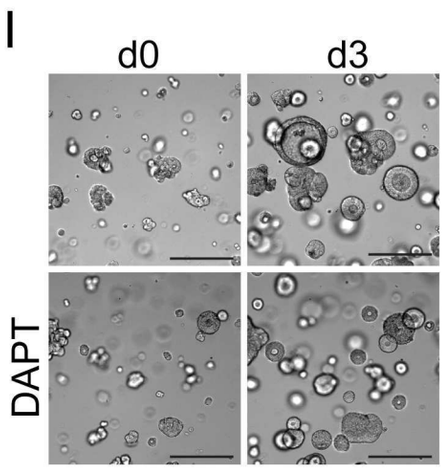

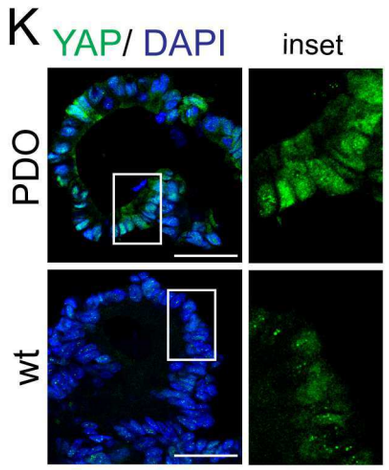

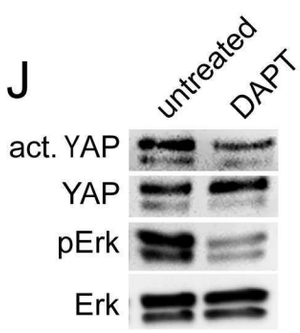

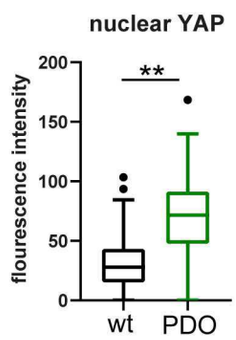

suppl. Fig. 5, Heuberger et al. 2021

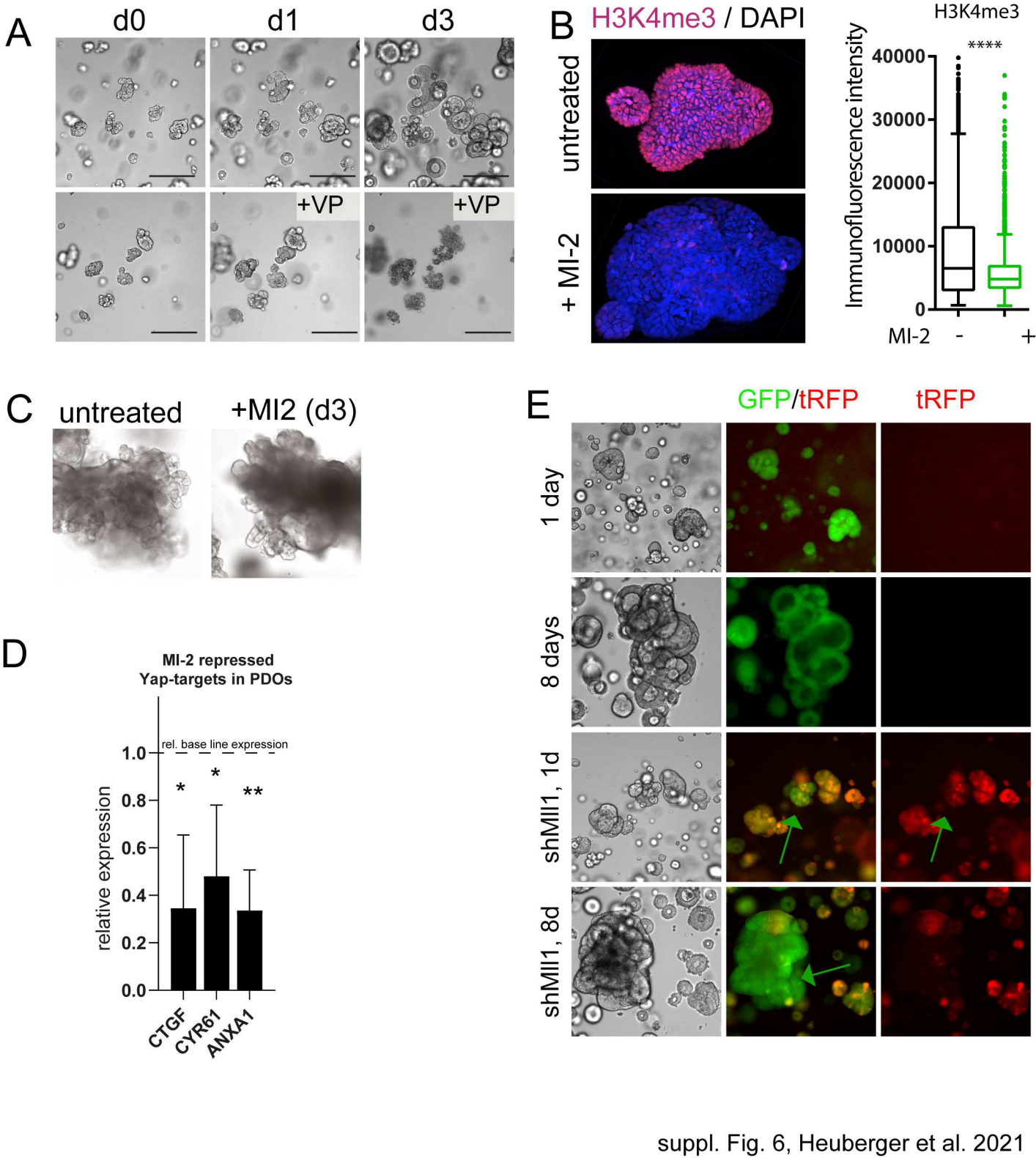

suppl. Fig. 6, Heuberger et al. 2021